

Measurement of the High-Frequency Spectrum of Ocean Surface Waves

HISASHI MITSUYASU

Research Institute for Applied Mechanics, Kyushu University, Hakozaki, Fukuoka 812, Japan

(Manuscript received 3 May 1977, in revised form 22 June 1977)

ABSTRACT

High-frequency spectra of wind-generated ocean waves were measured at an ocean research tower of Kyushu University using a fast-response wave recorder and an electronic differentiating circuit. Wind waves generated by a northeast wind (speed $U_{10.5}=8\text{ m s}^{-1}$, fetch $F=2\text{ km}$) were superimposed on the swell from the north and in a stationary state.

The equilibrium range of the wave spectrum, where the spectral form is given by

$$\phi(f) = (2\pi)^{-4} \beta g^2 f^{-5},$$

was clearly observed in a frequency range $f_m < f \leq 4\text{ Hz}$ of the measured spectrum, where g is the acceleration of gravity and f_m the spectral peak frequency. The measured value of the equilibrium constant β was 0.016 for the dimensionless fetch $\bar{F} (=gF/U_*^2) = 1.3 \times 10^6$ (where U_* is the friction velocity of the wind), which was very close to the value obtained by Burling (1959).

However, the equilibrium spectrum of the gravity wave range occurred only below 4 Hz, and the spectral form in the gravity-capillary range ($f > 5\text{ Hz}$) was given approximately by

$$\phi(f) = (2\pi)^{-5} \alpha_g g_* U_* f^{-4},$$

$$g_* = g + \gamma k^2, \quad \gamma = \sigma/\rho_w,$$

where σ is the surface tension, ρ_w the density of water and k the wavenumber. The measured value of the dimensionless constant α_g was 0.012 for the frequency range $6\text{ Hz} \leq f \leq 14\text{ Hz}$ of the measured spectrum, which was very close to the values measured in our laboratory experiment ($U_* \approx 40\text{ cm s}^{-1}$ at $F=5.85\text{ m}$ and 8.25 m). The result confirmed that the spectral form in the gravity-capillary range is really independent of the fetch.

1. Introduction

Recently much attention has been focused on the fine-structure of the high-frequency spectra of wind-generated waves. For example, the theory of radar sea return, which can be applied to remote sensing of the sea surface, needs detailed information on the structure of the high-frequency components of wind waves in the gravity-capillary range. In a recent paper, Pierson and Stacy (1973) proposed a spectral form for a very wide frequency range using many reports and data sources. They showed that the capillary range of the wave spectrum is strongly wind speed dependent but independent of the fetch. Independently, Toba (1973) proposed a high-frequency wave spectrum which gives frequency and wind speed dependence as $U_* f^{-4}$, where f is the frequency of the spectral component and U_* the friction velocity of the wind. In order to confirm the results obtained by Pierson and Stacy (1973) and by Toba (1973), we obtained in our previous study (Mitsuyasu and Honda, 1974) accurate measurements of the high-frequency spectra of wind-generated waves in a laboratory tank. Important findings of that study were as follows. The spectral density in the high-frequency range (~ 10 to 50 Hz) is strongly wind-

speed dependent as shown by Pierson and Stacy (1973) and the spectral form in that range is fairly close to the spectral form proposed by Toba (1973), although some systematic deviations from the proposed spectrum has been observed. Although the spectral form in the gravity-capillary range seemed to be independent of the fetch F in our previous study, definite conclusions were not obtained due to the short limited fetches (~ 1.05 to 8.25 m) of the wave tank.

One of the main purposes of the present study is to confirm the results of our previous laboratory study by using reliable data for the high-frequency spectra of ocean surface waves. In particular, we intend to clarify the effect of fetch on the high-frequency spectra in the gravity-capillary range.

Another controversial problem for the high-frequency spectra of wind-generated waves is concerned with the equilibrium range in wave spectra for the gravity wave range. Phillips (1958) showed, from the consideration of limiting configurations of surface waves, that an equilibrium range may exist, and by similarity considerations, he derived the spectral form

$$\phi(f) = (2\pi)^{-4} \beta g^2 f^{-5}, \quad (1)$$

where β is a universal constant usually called the equilibrium constant and g the acceleration of gravity. In a general sense, various observations of wave spectra in laboratory tanks and in the ocean supported the spectral form (1). However, several recent studies showed that the equilibrium constant β is not constant but decreases with increasing dimensionless fetch $\hat{F} = gF/U_*^2$ (Mitsuyasu, 1969; Liu, 1971; Hasselmann *et al.*, 1973). The observed values for the frequency exponent scattered around -5 , and in some cases were rather close to -4 . It is a little curious that such a relatively simple phenomenon has not been clarified so as to produce a definite conclusion. The situation is as follows: In the spectra of laboratory wind waves the spectral peak frequency f_m is relatively high, say, ~ 2 to 3 Hz, and the nonlinear effect of the spectral components near the frequency f_m affects the high-frequency side of the spectrum producing secondary and tertiary small peaks near $2f_m$ and $3f_m$ (Tick, 1959; Mitsuyasu, 1969). In the higher frequency region, $f > 3f_m$, the capillary effect increases gradually. Therefore, an accurate determination of the equilibrium range in wave spectra for the gravity wave range is relatively difficult in laboratory tanks. On the other hand, as emphasized by DeLeonibus *et al.* (1974), "no wave-measuring system approach used in the open ocean possesses the necessary frequency response, resolution, and accuracy required to record both large-amplitude low-frequency waves and small-amplitude high-frequency waves, which are generally superimposed on the larger waves".

In order to solve these difficulties, we have used in this study a resistance-type wave gage which has a sufficiently wide frequency response (0 to 30 Hz), and electronic differentiators combined with low-pass filters ($f_c = 17.8$ Hz). The output of the wave gage is differentiated twice before recording, and the wave signal $\eta(t)$, the differentiated signal $\dot{\eta}(t)$ and the twice-differentiated signal $\ddot{\eta}(t)$ are recorded simultaneously on a tape recorder. By this technique we were able to measure the high-frequency spectra of ocean waves very accurately up to 14 Hz.

2. Observing facility and equipments

a. Oceanographic research tower

Wind and waves were measured at an oceanographic research tower located 2 km northwest of Tsuyazaki, a fishing port which faces on the Tsushima Strait (Fig. 1). The water depth at the tower is 16 m and the bottom slope around the tower is relatively gentle ($\sim 1/300$). The research tower is a simple equilateral triangular platform which is composed essentially of three vertical piles (diameter 0.8 m) driven into the sea bottom at 7 m separation (Figs. 2 and 3). In order to reduce the influences of the tower, the wave gage and the cup anemometer were supported by a horizontal bar extending out ~ 3 m into the up-wind side of the tower (Fig. 2). The effects of wave disturbances reflected from the main piles of the tower were considered negligibly small at the location of the main wave gage.

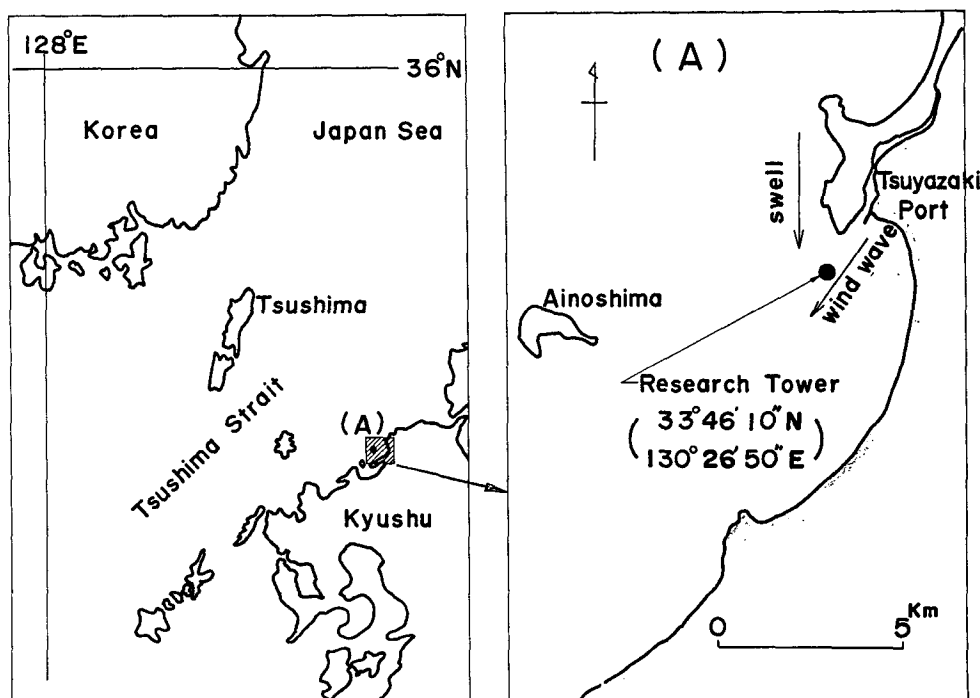


FIG. 1. Location of oceanographic research tower.

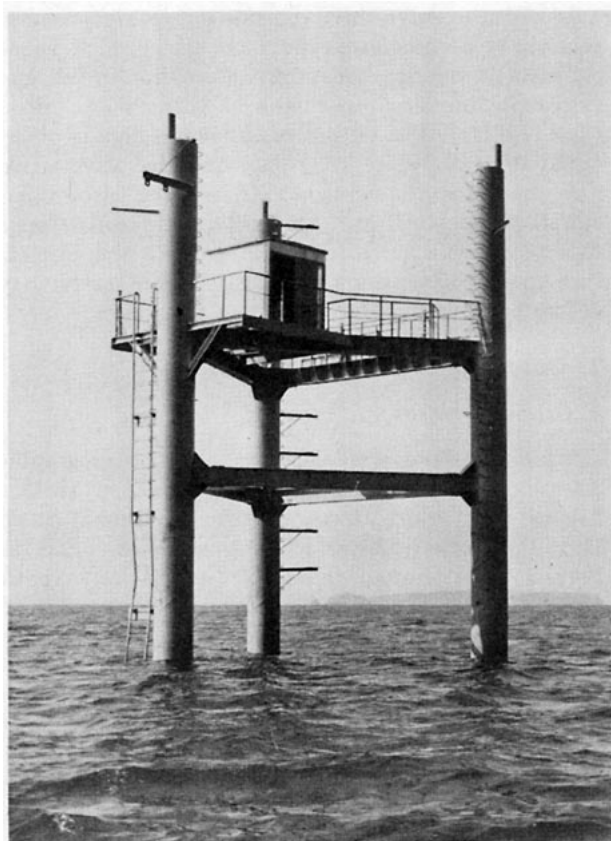


FIG. 2. Oceanographic research tower.

b. Wave gages

Waves were measured by a resistance-type wave gage which was specially designed to measure the high-frequency wave spectrum. As shown in Figs. 3 and 4, the wave gage is composed of an electric probe of a single 0.35 mm diameter nichrome wire and an electronic circuit, including a bridge circuit. The frequency response of the wave gage was tested by using a calibration set-up which was almost the same as that used in a previous study (Mitsuyasu and Honda, 1974). The probe (nichrome wire) of the wave gage was oscillated vertically through the air-water interface by using a large loud-speaker system, and the output of the wave gage was compared with the amplitude detected by a differential transformer. The amplitude response factor was approximately unity up to 30 Hz. On the other hand, the amplitude response factor of the capacitance-type wave gage described later was unity only up to 2 Hz.

Waves also were measured by three capacitance-type wave gages (Denshi Kōgyō VM103) fixed to each pile of the tower with arms 1 m long so as to reduce the effect of the disturbances from the vertical piles. The capacitance-type wave gages form an equilateral triangular array of side 7 m, and can detect some directional properties of ocean surface waves. However,

the wave data measured by these gages were used only as reference data because the amplitude response factors of these gages were not sufficient for measuring the high-frequency part of the wave spectrum.

c. Differentiator

The high-frequency spectrum of wind-generated waves is roughly proportional to f^{-4} – f^{-5} . Thus the spectral density of the high-frequency component, say $10f_m$, is $(10^{-4}$ – $10^{-5}) \times \phi(f_m)$, where $\phi(f_m)$ is the spectral density of the spectral peak frequency f_m . For such small spectral densities many errors will be introduced from the wave recording system and the procedures of spectral computation. In order to obtain reliable data for the high-frequency part of such a low spectral density, electronic differentiators were used as a kind of prewhitening device. If the frequency spectrum of surface elevation $\eta(t)$ is $\phi_\eta(f)$, then the frequency spectrum of the differentiated signal $\dot{\eta}(t)$ is given by

$$\phi_{\dot{\eta}}(f) = (2\pi f)^2 \phi_\eta(f), \quad (2)$$

and that of the double-differentiated signal $\ddot{\eta}(t)$ is given by

$$\phi_{\ddot{\eta}}(f) = (2\pi f)^4 \phi_\eta(f). \quad (3)$$

Therefore, in a wave spectrum which is proportional to f^{-4} – f^{-5} for the surface elevation $\eta(t)$, the spectrum of the double-differentiated signal $\ddot{\eta}(t)$ is proportional to a constant– f^{-1} . The electronic differentiators used in the present study were almost the same as those used in our previous study (Mitsuyasu and Honda, 1974) except for the cutoff frequencies of the low-pass filters. The low-pass filters with a cutoff frequency 17.8 Hz were used to eliminate various high-frequency noises.

d. Measurements

Wind speed and its direction were measured by a wind vane located at the top of the tower, the height of which is 12.5 m above the sea surface. Wind speed at 1.5 m above the sea surface was also measured by using a small cup anemometer supported by a probe (Fig. 3).

Wave signals measured by three capacitance-type wave gages, $\eta_1(t)$, $\eta_2(t)$, $\eta_3(t)$; those measured by the resistance-type wave gage, $\eta(t)$, its differentiated signal $\dot{\eta}(t)$ and double-differentiated signal $\ddot{\eta}(t)$; and wind speed at $Z = 1.5$ m, $U_{1.5}(t)$ were recorded simultaneously on a FM data recorder, and some of the data [$\eta(t)$, $\dot{\eta}(t)$, $\ddot{\eta}(t)$] were monitored on a three-channel pen recorder. The frequency response of the data recorder is unity for a frequency range from 0 to 1.25 K Hz. The block diagram of the measuring system is shown in Fig. 5.

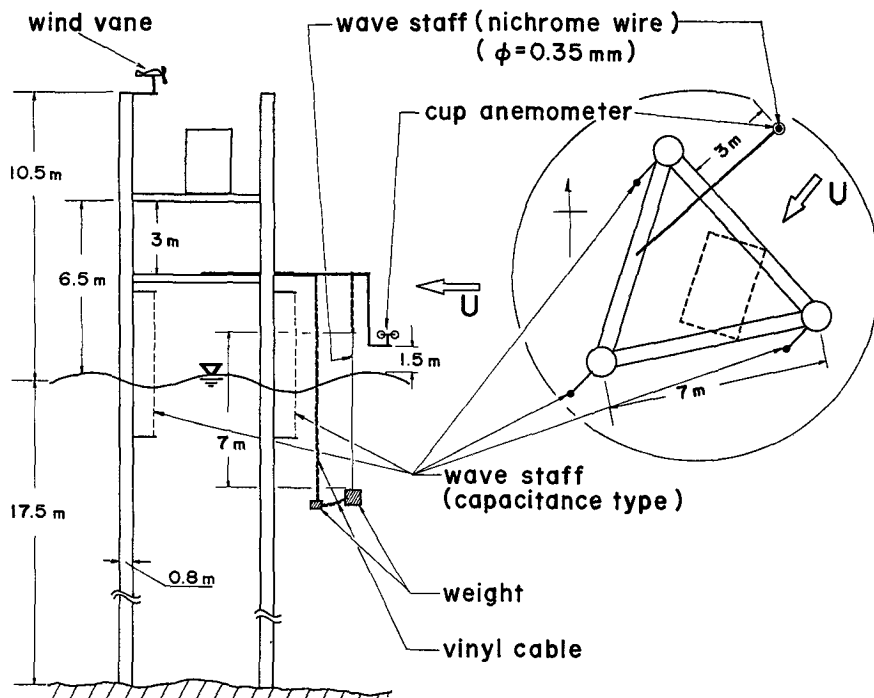


FIG. 3. Instrumentation scheme at the tower for wind and wave measurements.

3. Wave observations and data analysis

Waves were measured on 24 April 1976 from 1627 to 1657 (all times Japan Standard). From approximately 1400 to 1700 the wind continued to blow from the northeast maintaining a roughly constant speed ($8\text{--}10\text{ m s}^{-1}$). During the wave observation period, the mean wind speed was 8.0 m s^{-1} at $Z=10.5\text{ m}$ and 6.2 m s^{-1} at $Z=1.5\text{ m}$. If we assume a logarithmic distribution of the wind profile, the friction velocity of the wind becomes $U_* = 39\text{ cm s}^{-1}$. The fetch F from the upwind beach to the station is 2 km and the dimensionless fetch $\hat{F}(=gF/U_*^2)$ is 1.3×10^5 .

At the time of the wave observation, swell with approximately 7 s period and 0.5 m amplitude was coming from the north, and wind-generated waves from the northeast were superimposed on it. The wind-generated waves were roughly 1.7 s in mean period and 0.25 m in height, and they were breaking intermittently. The period and the height of the wind-generated waves were consistent with the fetch relations proposed by Mitsuyasu (1968).

Wave signals $\eta(t)$, $\dot{\eta}(t)$ and $\ddot{\eta}(t)$ and the wind speed $U_{1.5}(t)$ were recorded simultaneously on magnetic tape for 30 min . The data were then digitized through a high-speed A-D converter with a sampling frequency of 40 Hz , and each time series $(\eta, \dot{\eta}, \ddot{\eta}, U_{1.5})$ was divided into 32 subsamples each of which contained 2048 data points (length 51.2 s). Frequency spectra were computed by standard fast Fourier transform procedures. The final spectrum was obtained by taking moving averages

of three line spectra after taking a sample mean of the spectra of the 32 subsamples. Thus the equivalent degrees of each measured spectrum is ~ 192 . The confidence limits for the spectrum are very narrow. The limits of the 80% confidence band of the measured spectrum $\phi(f)$ are approximately $0.88\phi(f)$ and $1.15\phi(f)$.

4. Results

a. Wave records

A part of the wave record is shown in Fig. 6 and in Fig. 7 at a higher recording speed. The dashed line superimposed on the $\eta(t)$ record in Fig. 6 corresponds to swell which has been determined visually on the wave record. It can be seen from Fig. 6 that the swell is

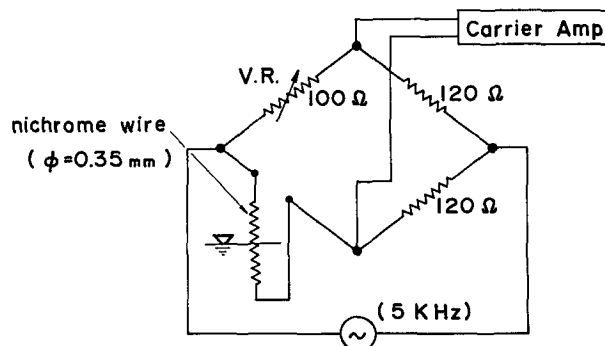


FIG. 4. Wave measuring circuit.

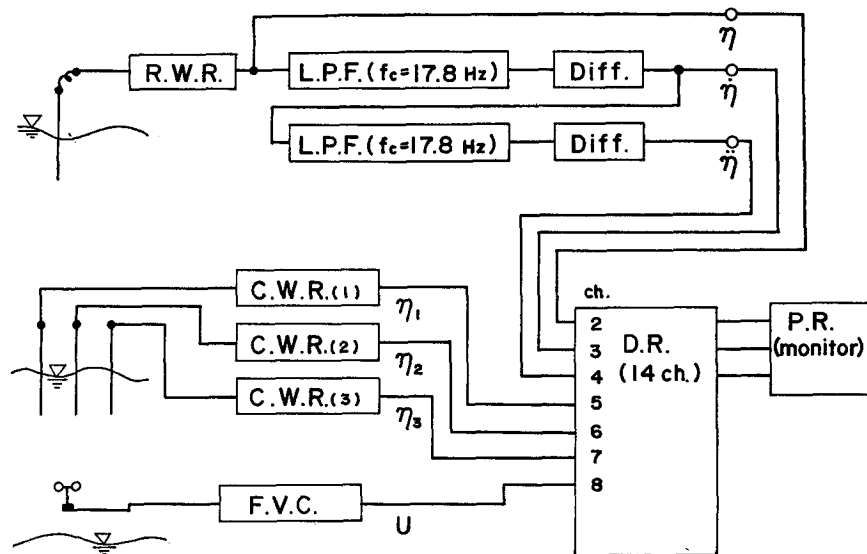


FIG. 5. General scheme of measuring system. R.W.R., resistance-type wave recorder; L.P.F., low-pass filter; Diff., differentiator; C.W.R., capacitance-type wave recorder; D.R., data recorder; P.R., pen recorder; F.V.C., frequency-voltage converter.

larger than the wind-generated waves in the record of $\eta(t)$, that the wind-generated wave is predominant in the record of $\dot{\eta}(t)$, and that capillary waves superimposed on the wind-generated waves are most predominant in the record of $\ddot{\eta}(t)$. Since the capillary waves can hardly be seen in the record of $\eta(t)$, the results of Figs. 6 and 7 show that the use of the differentiating circuit is very effective for detecting high-frequency waves superimposed on the large dominant waves. Furthermore, closer examination of the record of $\dot{\eta}(t)$ shows the very interesting property of the overlapping ripples that their amplitudes [actually the amplitudes of $\ddot{\eta}(t)$] change with the phase of the dominant wave. That is, when we compare the record of $\dot{\eta}(t)$ with that of $\eta(t)$, the amplitude of $\dot{\eta}(t)$ can be seen to be larger

at the crest of $\eta(t)$ and smaller at the trough of $\eta(t)$. The extremely large values of $\dot{\eta}(t)$ shown in Fig. 6 mean that wave breaking occurred at those times. Therefore, the electronic differentiating circuit can also be used for detecting breaking waves.

b. Wave spectra

Fig. 8 shows the frequency spectrum $\phi_{\eta}(f)$ of the surface elevation $\eta(t)$. The frequency spectra $\phi_{\dot{\eta}}(f)$ and $\phi_{\ddot{\eta}}(f)$ are shown in Figs. 9 and 10, respectively, where $\phi_{\dot{\eta}}(f)$ is the spectrum of the differentiated signal $\dot{\eta}(t)$, and $\phi_{\ddot{\eta}}(f)$ is the spectrum of the double-differentiated signal $\ddot{\eta}(t)$. In the upper part of each figure the frequency spectrum is shown on a linear scale, and the

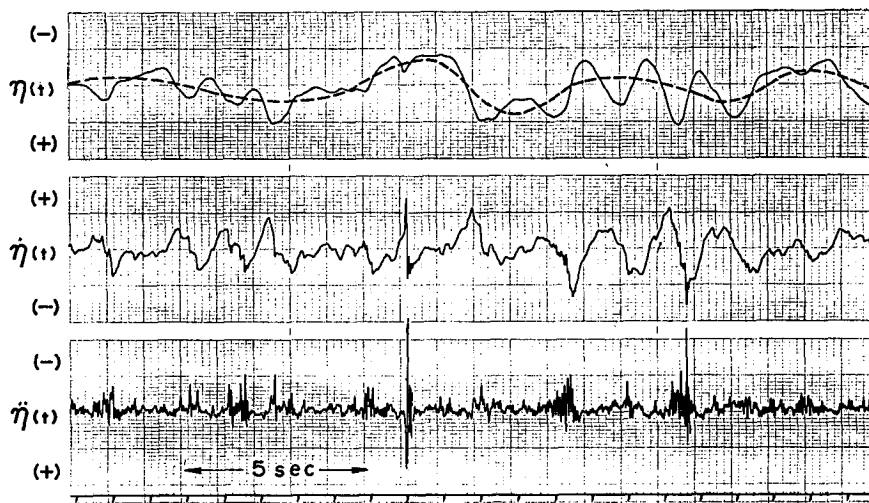


FIG. 6. Wave records, $\eta(t)$, $\dot{\eta}(t)$ and $\ddot{\eta}(t)$. Time increases to the right.

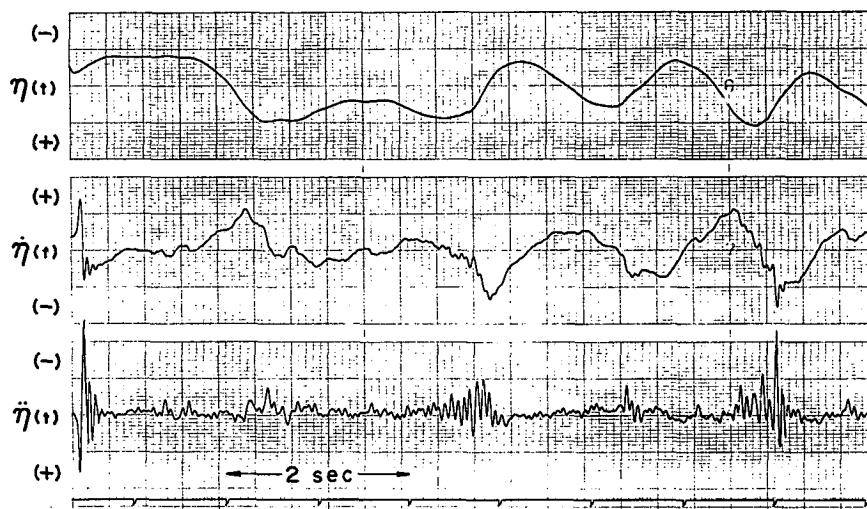


FIG. 7. As in Fig. 6 except for higher speed recording.

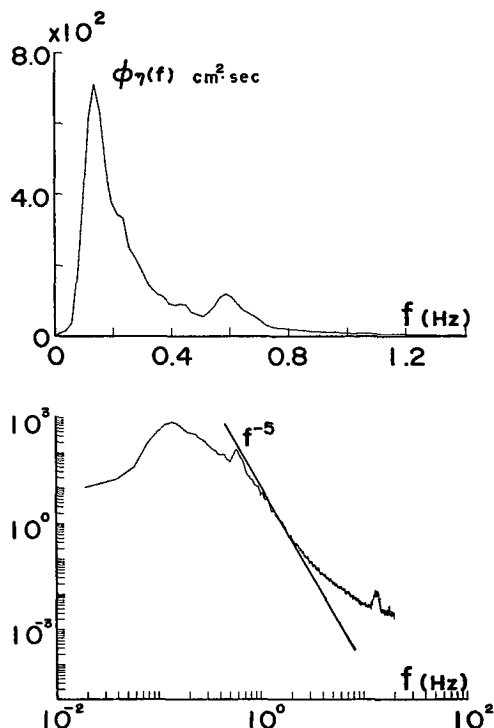
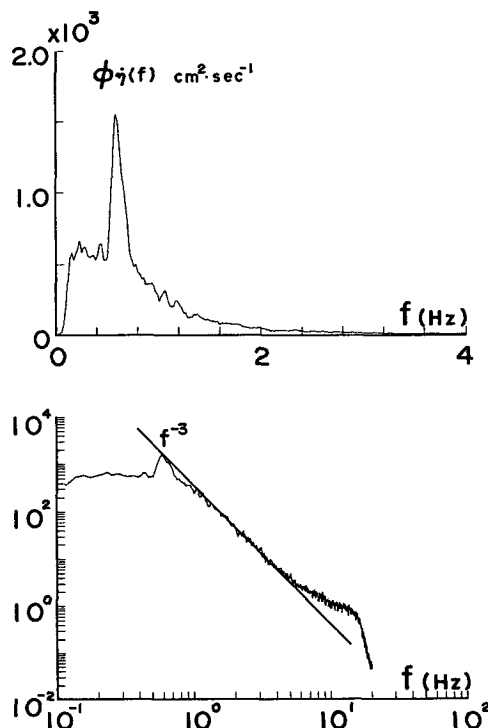
same spectrum is shown on a logarithmic scale in the lower part of the figure. The dominant peak of $\phi_\eta(f)$ at $f \approx 0.14$ Hz corresponds to the swell, the secondary small peak at $f \approx 0.6$ Hz corresponds to the wind-generated wave and the tertiary peak at $f \approx 13$ Hz is due to the noise of a generator used as a power source. It can be seen that the swell is higher than the wind-generated waves. However, in the spectra of the differentiated signals, which are shown in Figs. 9 and 10, the spectral densities of the wind-generated waves

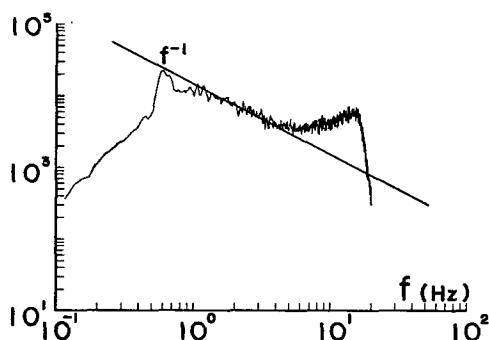
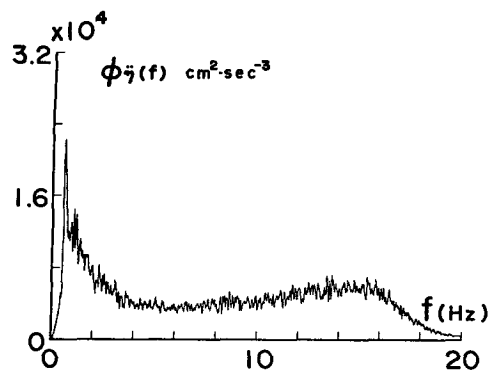
are much larger than that of the swell, and the generator noise is negligible.

The spectral densities of the differentiated signals, $\phi_{\dot{\eta}}(f)$ and $\phi_{\ddot{\eta}}(f)$, can be converted to the spectrum of the surface elevation $\phi_\eta(f)$ by using the following relations:

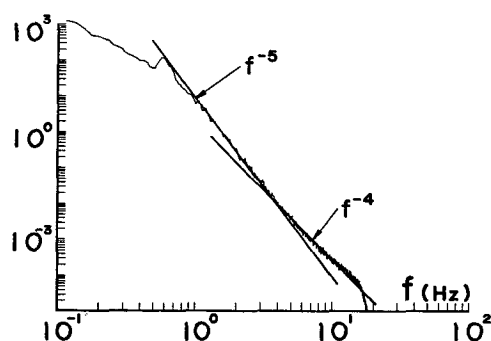
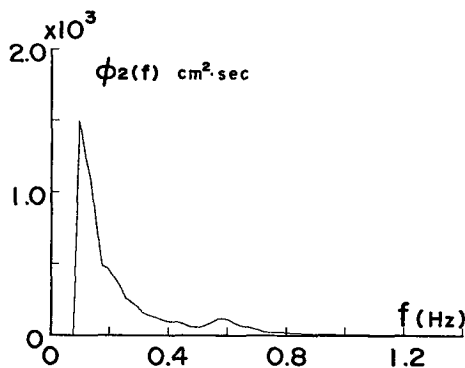
$$\phi_\eta(f) = (2\pi f)^{-2} \phi_{\ddot{\eta}}(f) \quad [= \phi_1(f)], \quad (4)$$

$$\phi_{\dot{\eta}}(f) = (2\pi f)^{-1} \phi_{\ddot{\eta}}(f) \quad [= \phi_2(f)]. \quad (5)$$

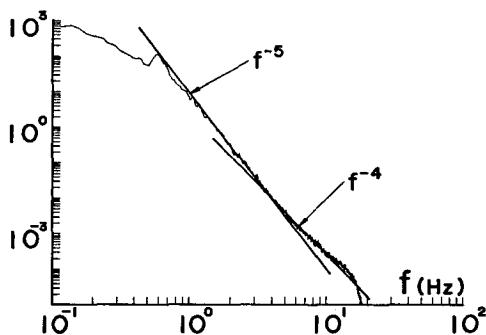
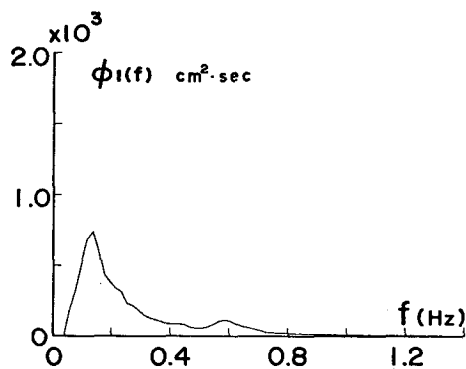
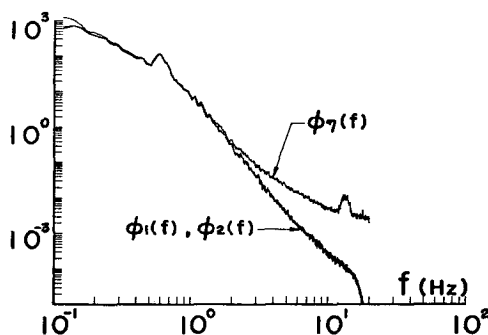
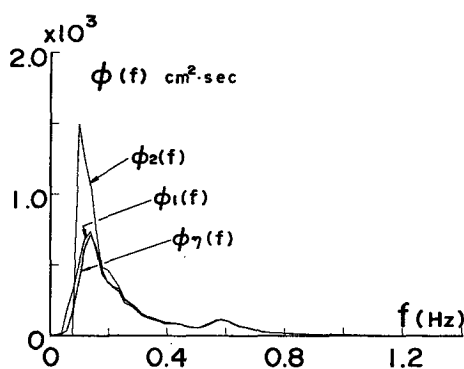

 FIG. 8. Frequency spectrum of surface elevation $\eta(t)$.

 FIG. 9. Frequency spectrum of differentiated signal $\dot{\eta}(t)$.

FIG. 10. Frequency spectrum of double-differentiated signal $\ddot{\eta}(t)$.

The converted spectra $\phi_1(f)$ and $\phi_2(f)$ are shown, respectively, in Figs. 11 and 12, and they are compared with $\phi_\eta(f)$ in Fig. 13. It can be seen from Fig. 13 that,

FIG. 12. As in Fig. 11 except for $\dot{\eta}(t)$.

in the dominant part of the wind wave spectra ($f=0.4$ – 1.0 Hz), the three spectra $\phi_\eta(f)$, $\phi_1(f)$ and $\phi_2(f)$ coincide quite well. However, for the high-frequency region of

FIG. 11. Frequency spectrum of surface elevation determined from the differentiated signal $\dot{\eta}(t)$.FIG. 13. Comparison of three wave spectra determined, respectively, from $\eta(t)$, $\dot{\eta}(t)$ and $\ddot{\eta}(t)$.

the spectra ($f \gtrsim 2$ Hz), $\phi_{\eta}(f)$ deviates gradually from the other two spectra with increasing frequency although $\phi_1(f)$ and $\phi_2(f)$ coincide almost perfectly in the high-frequency region.

The deviation of $\phi_{\eta}(f)$ from $\phi_1(f)$ and $\phi_2(f)$ can be attributed partly to the effect of noise in the measuring system, and in particular to the noise in the data recording system. The spectral density of white noise of the order 10^{-3} (in the same units as the wave spectrum) was obtained by analyzing the reproduced magnetic tape signals at the time calibration signals (dc signals) were recorded. On the other hand, the levels of the white noise spectra for the differentiated signals are 10^{-2} for $\phi_{\dot{\eta}}(f)$ and 10^1 for $\phi_{\ddot{\eta}}(f)$ in the same units as the corresponding wave spectra. Compared to the spectral densities shown in Figs. 9 and 10, the effects of these noises are negligible for the spectra of the differentiated signals $\phi_{\dot{\eta}}(f)$ and $\phi_{\ddot{\eta}}(f)$.

Although the noise in the measuring system does affect the high-frequency part ($f > 6$ Hz) of the measured spectrum $\phi_{\eta}(f)$, it is not sufficient for explaining the deviation of $\phi_{\eta}(f)$ from $\phi_1(f)$ or $\phi_2(f)$, which becomes noticeable at $f \approx 2$ Hz. Thus the value of $\phi_{\eta}(f)$ at $f = 2$ Hz is $\sim 10^{-1} \text{ cm}^2 \text{ s}^{-1}$ and it is much larger than the corresponding value of the noise ($10^{-3} \text{ cm}^2 \text{ s}^{-1}$). After various checks of sources of the error, it has been found that the error in the measured wave spectrum $\phi_{\eta}(f)$ is largely due to the leakage effect in the spectral computation, and it can be reduced, to a certain extent, by using the data window. On the other hand, the leakage effect for $\phi_1(f)$ or $\phi_2(f)$ is negligible due to the prewhitening effects of the differentiation of the signal.

Here again we can see the advantages of the electronic differentiating circuit for measuring the high-frequency wave spectrum. The sharp fall of the spectral density at $f > 15$ Hz is attributed to the effect of the low-pass filters (cutoff frequency $f_c = 17.8$ Hz).

From the results discussed above, the frequency spectrum $\phi_2(f) [= (2\pi f)^{-4} \phi_{\ddot{\eta}}(f)]$ will be used hereafter for discussion of the high-frequency spectra. Almost the same conclusion can be obtained from the data for $\phi_1(f) [= (2\pi f)^{-2} \phi_{\dot{\eta}}(f)]$, because, as readily seen from Figs. 11, 12 and 13, $\phi_1(f)$ coincides almost exactly with $\phi_2(f)$ for the high-frequency part of the spectra.

Finally, a brief discussion should be added on the effect of the differentiating circuit on the low-frequency part of the wave spectrum. As can be seen from (4) and (5), the spectral densities of the low-frequency components are much suppressed in the differentiated signals. Therefore, various kinds of low-frequency noise will affect the low-frequency part of the spectrum. In fact, as shown in Fig. 13, the spectral form of the swell determined from $\eta(t)$ [i.e., $\phi_2(f)$ in the frequency range $0 \sim 0.4$ Hz] is much different from that determined from $\dot{\eta}(t)$ or $\ddot{\eta}(t)$.

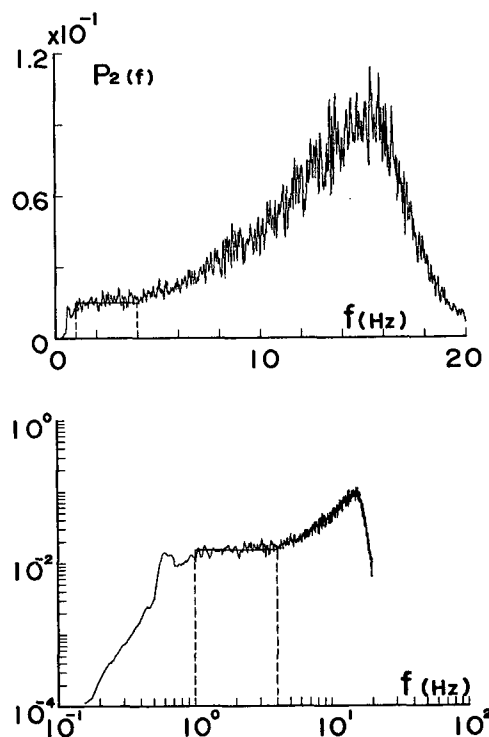


FIG. 14. Normalized form of the equilibrium spectrum of wind-generated waves, $P_2(f) = (2\pi)^4 g^{-2} f^5 \phi_2(f)$.

5. Equilibrium range in the spectra of wind-generated waves

As shown in Figs. 11 and 12, the spectral density is proportional to f^{-5} for a frequency range from 0.6 to 4 Hz, and it is roughly proportional to f^{-4} for the higher frequency range, $f > 4$ Hz. In order to investigate these spectral forms more quantitatively, the measured spectrum $\phi_2(f)$ has been normalized first to the form

$$P_2(f) = (2\pi)^4 g^{-2} f^5 \phi_2(f) [= f g^{-2} \phi_{\ddot{\eta}}(f)], \quad (6)$$

and it is shown in Fig. 14. It can be seen that the normalized spectrum shows an almost exactly constant value over the frequency range 1–4 Hz. Therefore, the equilibrium spectrum of the form (1) does exist in some high-frequency region of the wave spectrum. The equilibrium constant β , which is determined as the average value of $P_2(f)$ in the frequency range 1–4 Hz, is $\beta = 0.0162$. When we recall the fact that the dimensionless fetch for the present case is $\hat{F} = 1.3 \times 10^5$, the above value of β can be compared with the data obtained by Burling (1959), i.e.,

$$\beta = 0.0148 \quad \text{for } \hat{F} = 1.1 \times 10^5,$$

and with our previous data measured at Hakata Bay (Mitsuyasu, 1969),

$$\beta = 0.0122 \quad \text{for } \hat{F} = 6.1 \times 10^5.$$

These results show that the equilibrium constant β measured in our present study is very close to that

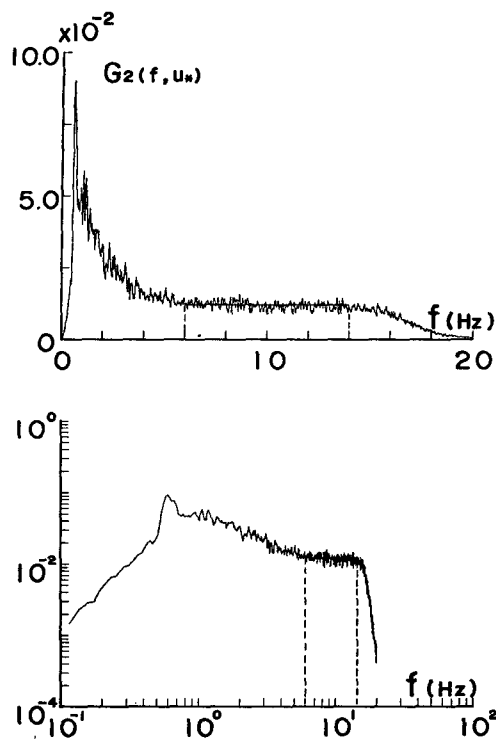


FIG. 15. Normalized form of the gravity-capillary spectrum $G_2(f, U_*) = (2\pi)^3 U_*^{-1} g_*^{-1} f^4 \phi_2(f)$ of wind-generated waves.

measured by Burling (1959) for the case of almost the same dimensionless fetch, and that the equilibrium constant decreases with increasing dimensionless fetch as mentioned previously by Longuet-Higgins (1969), Mitsuyasu (1969) and Hasselmann *et al.* (1973).

The effect of swell on the equilibrium form of wind wave spectra, discussed recently Kitaigorodskii *et al.* (1975), is not clear in our present data. This may be attributed to the small steepness ($H/L \sim 0.01$) of the swell.

6. Spectral form of the gravity-capillary range

According to our previous study (Mitsuyasu and Honda, 1974), the spectral density in the gravity-capillary range is clearly wind speed dependent as mentioned first by Pierson and Stacy (1973) with a form given approximately by

$$\phi(f) = (2\pi)^{-3} \alpha_g U_* g_* f^{-4}, \quad (7)$$

$$g_* = g + \gamma k^2, \quad \gamma = \sigma / \rho_w, \quad (8)$$

where k is the wavenumber ($=2\pi/L$), σ the surface tension of the water, ρ_w the density of the water and α_g a dimensionless constant which seems to depend on the wind speed. The spectral form (7) was originally presented by Toba (1973) as an extended form of the high-frequency wave spectrum in the gravity wave range which was applicable to the gravity-capillary range. Although the spectral form of this gravity-

capillary range seemed to be independent of the fetch, a definite conclusion was not obtained in our previous study due to the short limited range of the fetch ($F=1.05-8.25$ m). By using the present data for the high-frequency spectrum of ocean waves measured for a large fetch $\bar{F}=1.3 \times 10^5$, the spectral form and its dependence on the dimensionless fetch \bar{F} can be investigated.

By taking the spectral form (7) into account, the measured spectrum has been normalized to the form

$$G_2(f, U_*) = (2\pi)^3 U_*^{-1} g_*^{-1} f^4 \phi_2(f) = (2\pi U_*)^{-1} g_* \phi_{\bar{g}}(f). \quad (9)$$

It should be mentioned here that g_* is a function of the frequency f , because g_* contains the wavenumber k and k is related to the frequency f through the dispersion relation. However, since we have had no reliable form of the dispersion relation for gravity-capillary waves coexisting with drift current and swell, we have tentatively used the ordinary dispersion relation for the free linear waves in the gravity-capillary range,

$$(2\pi f)^2 = gk + \gamma k^3. \quad (10)$$

The measured spectrum normalized in the form (9) is shown in Fig. 15. It can be seen that the normalized spectral density is almost constant in the frequency range $5 \text{ Hz} < f \leq 14 \text{ Hz}$. This means that the spectral form (7) is a very accurate approximation to the measured spectrum in the gravity-capillary range. Since the spectral density for $f > 14 \text{ Hz}$ is affected by the low-pass filters, the high-frequency limit of this range is not necessarily limited to 14 Hz. The constant α_g , which is determined as the average value of $G_2(f)$ in a frequency range $6 \text{ Hz} \leq f \leq 14 \text{ Hz}$, is

$$\alpha_g = 0.012.$$

This value of α_g is very close to the previous values

$$\alpha_g = 0.011-0.012$$

which were determined for a similar wind speed $U_* \approx 40 \text{ cm s}^{-1}$ but for the very short different fetches $F=5.85-8.25$ m (Mitsuyasu and Honda, 1974). It can be said that the spectral form in the gravity-capillary range is given very accurately by (7) and its form is almost independent of the fetch F . In other words, the spectral form in the gravity-capillary range is unaffected by the existence of the large dominant waves in the gravity range. It is also seen from Fig. 15 that the spectral form in the range $f < 5 \text{ Hz}$ deviates clearly from the form (7), as would naturally be expected from the results in Section 5. Therefore, the high-frequency part of the wind wave spectrum can be divided at least into two typical regions: the gravity equilibrium range ($f_m < f < 4 \text{ Hz}$), where the spectral form is given by the equilibrium form (1), and the gravity-capillary range ($6 \text{ Hz} < f < f_u$), where the spectral form is given by (7). The upper limit f_u of the gravity-capillary range is undetermined in the present study but is at least larger

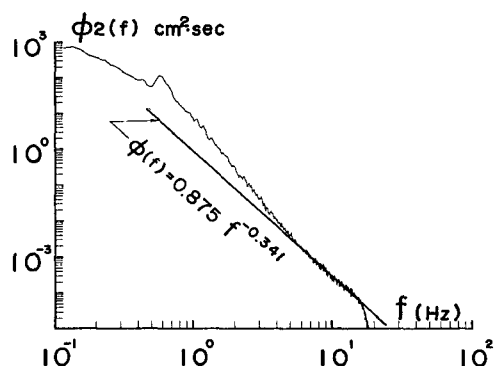


FIG. 16. Comparison of the frequency spectrum of surface elevation $\phi_2(f)$ with Eqs. (11) and (12) for $U_* = 35 \text{ cm s}^{-1}$.

than 14 Hz. The frequency range $4 \text{ Hz} < f < 6 \text{ Hz}$ can be considered as a kind of transition range.

Quite recently, Pierson (1976) proposed a new empirical formula for high-frequency spectra of wind-generated waves, on the basis of our previous data (Mitsuyasu and Honda, 1974). The proposed form of the spectrum is given by

$$\phi(f) = A(f/f_0)^{-p}, \quad (11)$$

where

$$\left. \begin{aligned} p &= 5.17 - 1.1 \log_{10} U_* \\ f_0 &= 1 \text{ Hz} \end{aligned} \right\}. \quad (12)$$

Although further discussion seems to be required on dimensional grounds, this formula gives a good fit to our previous data. Fig. 16 compares our present data with Eq. (11). The agreement is quite satisfactory for the present data, too.

7. Conclusions

The high-frequency spectrum of the ocean surface waves in a steady state was measured accurately up to 14 Hz. The main findings are as follows:

1) The gravity equilibrium from (1) of the spectra of wind-generated waves was clearly observed in a frequency range $f_m < f \lesssim 4 \text{ Hz}$. The equilibrium constant β was very close to that measured by Burling (1959). The equilibrium range of the spectra seemed to be unaffected by the swell obliquely crossing the wind-generated waves.

2) The form of the ocean wave spectrum in the frequency range $6 \text{ Hz} < f < f_u$, was very close to the spectral form (7) in the gravity-capillary range, which had been confirmed for laboratory wind waves (Mitsuyasu and Honda, 1974). Another empirical formula (11) derived by Pierson (1976) from our laboratory data (Mitsuyasu and Honda, 1974) also fits the present data in the gravity-capillary range. Therefore, the spectral form in the gravity-capillary range can be considered to be independent of the fetch or the scales of dominant waves. The high-frequency limit f_u of this range was undetermined in this study, but it should be larger than 14 Hz.

Although the accuracy of the measured data is very high, the data of this study are limited to the case of a wind speed $U_{10.5} = 8 \text{ m s}^{-1}$. Further observations for different wind speeds will be needed for a complete check of our previous study in a laboratory tank. Discussions of physical mechanisms interpreting the results reported here are deferred to a subsequent paper.

Acknowledgments. The author appreciates the invaluable comments of Profs. W. J. Pierson, O. M. Phillips, Y. Toba and K. Hasselmann. The author is indebted to Mr. K. Eto, Mr. T. Honda and Mr. A. Masuda for their assistance in the wave observation, to Mr. M. Tanaka for computer analysis of the wave data, and to Miss N. Uraguchi for typing the manuscript.

The work was supported by the science fund from the Ministry of Education. The ocean research tower used in the present study was constructed under a grant from the Ministry of Education for a special project entitled "A field study of ocean research platforms". The analysis of the wave data was made on FACOM 230-48 computer system at Research Institute for Applied Mechanics.

REFERENCES

- Burling, R. W., 1959: The spectrum of waves at short fetches. *Dtsch. Hydrogr. Z.*, **12**, 45-64, 96-117.
- DeLeonibus, P. S., L. S. Simpson and M. G. Mattie, 1974: Equilibrium range in wave spectra observed at an open-ocean tower. *J. Geophys. Res.*, **79**, 3041-3053.
- Hasselmann, K. et al., 1973: Measurements of wind-wave growth and swell decay during the Joint North Sea Wave Project (JONSWAP). *Dtsch. Hydrogr. Z.*, **12**, 1-95.
- Kitaigorodskii, S. A., V. P. Krasitskii and M. M. Zaslavskii, 1975: On Phillips' theory of equilibrium range in the spectra of wind-generated gravity waves. *J. Phys. Oceanogr.*, **5**, 410-420.
- Liu, P. C. 1971: Normalized and equilibrium spectra of wind waves in Lake Michigan. *J. Phys. Oceanogr.*, **1**, 249-257.
- Longuet-Higgins, M. S. 1969: On wave breaking and the equilibrium spectrum of wind-generated waves. *Proc. Roy. Soc. London*, **A310**, 151-159.
- Mitsuyasu, H. 1968: On the growth of the spectrum of wind-generated waves (I). *Rep. Res. Inst. Appl. Mech., Kyushu Univ.*, **16**, 459-482.
- , 1969: On the growth of the spectrum of wind-generated waves (II). *Rep. Res. Inst. Appl. Mech., Kyushu Univ.*, **18**, 235-248.
- , and T. Honda, 1974: The high frequency spectrum of wind-generated waves. *J. Oceanogr. Soc. Japan*, **30**, 185-198.
- Phillips, O. M., 1958: The equilibrium range in the spectrum of wind-generated waves. *J. Fluid Mech.*, **4**, 426-434.
- Pierson, W. J., 1976: The theory and applications of ocean wave measuring systems at and below the sea surface, on the land, from air craft. NASA Contractor Rep. CR-2646, 400 pp.
- , and R. A. Stacy, 1973: The elevation, slope and curvature spectra of wind roughened sea surface. NASA Contractor Rep. CR-2247, 128.
- Tick, L. J., 1959: A non-linear random model of gravity waves I. *J. Math. Mech.*, **8**, 643-651.
- Toba, Y., 1973: Local balance in the air-sea boundary process III. *J. Oceanogr. Soc. Japan*, **29**, 209-225.